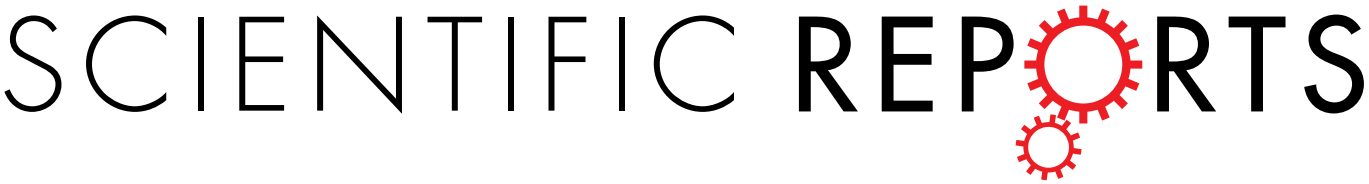

OPEN

Critical phenomenon of the near room temperature skyrmion material FeGe

Received: 02 December 2015
Accepted: 11 February 2016
Published: 29 February 2016

Lei Zhang[1], Hui Han[1,2], Min Ge[3], Haifeng Du[1], Chiming Jin[1], Wensen Wei[1], Jiyu Fan[4], Changjin Zhang[1], Li Pi[1,3] & Yuheng Zhang[1,3]

The cubic B20 compound FeGe, which exhibits a near room temperature skyrmion phase, is of great importance not only for fundamental physics such as nonlinear magnetic ordering and solitons but also for future application of skyrmion states in spintronics. In this work, the critical behavior of the cubic FeGe is investigated by means of bulk dc-magnetization. We obtain the critical exponents ($\beta = 0.336 \pm 0.004$, $\gamma = 1.352 \pm 0.003$ and $\beta = 5.276 \pm 0.001$), where the self-consistency and reliability are verified by the Widom scaling law and scaling equations. The magnetic exchange distance is found to decay as $J(r) \approx r^{-4.9}$, which is close to the theoretical prediction of 3D-Heisenberg model (r^{-5}). The critical behavior of FeGe indicates a short-range magnetic interaction. Meanwhile, the critical exponents also imply an anisotropic magnetic coupling in this system.

In recently years, skyrmion state, which is a topologically protected nanoscale vortex-like spin structure, has attracted great interest due to its potential application in spintronic storage function[1–12]. It has been demonstrated that the skyrmion phase is thermodynamically stable magnetic vortex state in magnetic crystals[13,14]. In addition, writing and deleting single magnetic skyrmion have been realized in PdFe bilayer on Ir(111) surface[15,16]. These findings pave a significant path to design quantum-effect devices based on the tunable skyrmion dynamics. The room-temperature skyrmion materials hosting stable skrymion phase are paid considerable attention[17]. The cubic FeGe belongs to the space group $P2_13$, in which the non-centrosymmetric cell results in a weak Dzyaloshinskii-Moriya (DM) interaction. The competition of DM interaction between the much stronger ferromagnetic exchange finally causes a long modulation period of a helimagnetic ground state[1,2,18]. A bulk FeGe sample exhibits a long-range magnetic order at Curie temperature $T_C = 278.2$ K, and displays a complex succession of temperature-driven crossovers in the vicinity of T_C[19,20]. The skyrmion phase emerges in a narrow temperature range just below T_C in the filed range from 0.15 to 0.4 kOe. The existence of the near room temperature skyrmion phase in FeGe, to our knowledge the highest T_C in B20 skyrmion compounds, makes it one of the most promising candidate of the next generation spintronic devices. Recently, more stable skyrmion phase has been realized in FeGe thin film, and it has been claimed that the skyrmions can be tuned by the crystal lattice[21–23]. On the other hand, multiple and complex magnetic interactions have also been found in FeGe. An inhomogeneous helimagnetic state has been discovered above T_C due to the strong precursor phenomena[19,24]. More interestingly, it has been revealed that the helical axis (q-vector direction) orientates depending on temperature. At zero magnetic field, the helical axis is along the <100> direction below 280 K. With decreasing temperature, it changes to the <111> direction at 211 K[20].

In view of the potential application and abundant physics in FeGe, a deep investigation of its magnetic exchange is of great importance not only for fundamental physics such as nonlinear magnetic ordering and solitons but also for creation of a basic for future application of skyrmion states and other chiral modulations in spintronics. In this work, the critical behavior of FeGe has been investigated by means of bulk dc-magnetization. The critical exponents ($\beta = 0.336 \pm 0.004$, $\gamma = 1.352 \pm 0.003$, and $\delta = 5.267 \pm 0.001$) are obtained, where the self-consistency and reliability are verified by the Widom scaling law and the scaling equations. These critical

[1]High Magnetic Field Laboratory, Chinese Academy of Sciences, Hefei 230031, China. [2]University of Science and Technology of China, Hefei 230026, China. [3]Hefei National Laboratory for Physical Sciences at the Microscale, University of Science and Technology of China, Hefei 230026, China. [4]Department of Applied Physics, Nanjing University of Aeronautics and Astronautics, Nanjing 210016, China. Correspondence and requests for materials should be addressed to L.Z. (email: zhanglei@hmfl.ac.cn)

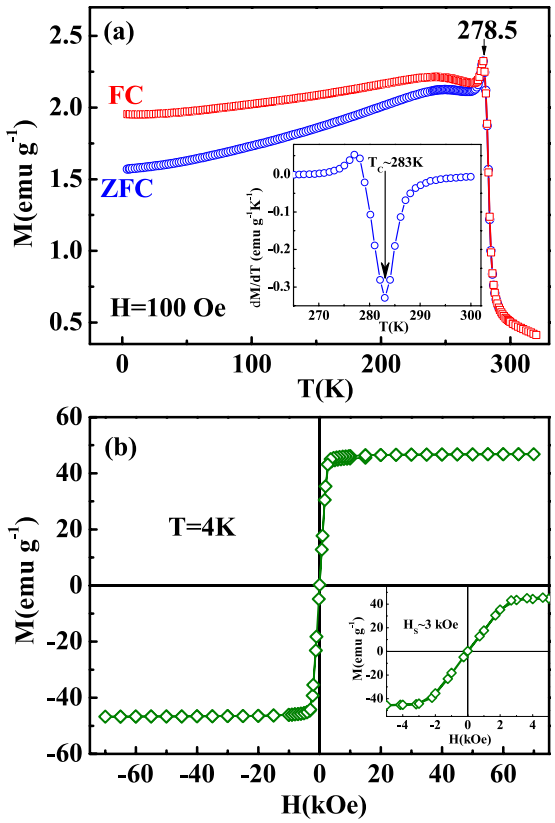

Figure 1. (**a**) The temperature dependence of magnetization $[M(T)]$ for FeGe under $H = 100$ Oe [the inset shows the derivative magnetization (dM/dT) vs T]; (**b**) the isothermal magnetization $[M(H)]$ at 4 K (the inset gives the magnified region in the lower field regime).

behavior of FeGe indicates a short-range magnetic interaction with a magnetic exchange distance decaying as $J(r) \approx r^{-4.9}$. The obtained critical exponents also imply an anisotropic magnetic coupling in FeGe system.

Results and Discussion

It is well known that the critical behavior for a second-order phase transition can be investigated through a series of critical exponents. In the vicinity of the critical point, the divergence of correlation length ξ leads to universal scaling laws for the spontaneous magnetization M_S and initial susceptibility χ_0. Subsequently, the mathematical definitions of the exponents from magnetization are described as[25,26]:

$$M_S(T) = M_0(-\varepsilon)^{\beta}, \ \varepsilon < 0, T < T_C \tag{1}$$

$$\chi_0^{-1}(T) = (h_0/M_0)\varepsilon^{\gamma}, \ \varepsilon > 0, T > T_C \tag{2}$$

$$M = DH^{1/\delta}, \ \varepsilon = 0, T = T_C \tag{3}$$

where $\varepsilon = (T - T_C)/T_C$ is the reduced temperature; M_0/h_0 and D are the critical amplitudes. The parameters β (associated with M_S), γ (associated with χ_0), and δ (associated with T_C) are the critical exponents. Universally, in the asymptotic critical region ($|\varepsilon| < 0.1$), these critical exponents should follow the Arrott-Noakes equation of state[27]:

$$(H/M)^{1/\gamma} = (T - T_C)/T_C + (M/M_1)^{1/\beta} \tag{4}$$

Therefore, the critical exponents β and γ can be obtained by fitting the $M_S(T)$ and $\chi_0^{-1}(T)$ curves using the modified Arrott plot of $M^{1/\beta}$ vs $(H/M)^{1/\gamma}$. Meanwhile, δ can be generated directly by the $M(H)$ at the critical temperature T_C according to Eq. (3).

Generally, the critical temperature T_C can be roughly determined by the temperature dependence of magnetization $[M(T)]$. Figure 1(a) shows the $M(T)$ curves for FeGe under zero-field-cooling (ZFC) and field-cooling (FC) with an applied field $H = 100$ Oe. The $M(T)$ curves exhibit an abrupt decline with the increase of temperature, corresponding to the paramagnetic-helimagnetic (PM-HM) transition. A sharp peak is observed at $T = 278.5$ K. The inset of Fig. 1(a) gives dM/dT vs T, where $T_C \approx 283$ K is determined from the minimum of the dM/dT curve.

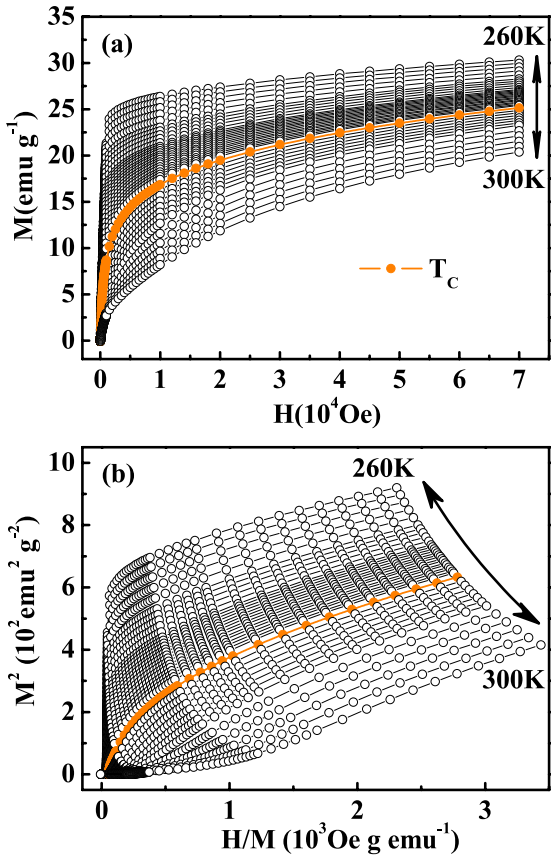

Figure 2. (**a**) The initial magnetization around T_C for FeGe; (**b**) Arrott plots of M^2 vs H/M [the $M(H)$ curves are measured at interval $\Delta T = 1$ K, and $\Delta T = 0.5$ K when approaching T_C].

Wilhelm *et al.* has demonstrated that a long-rang magnetic order occurs below 278.2 K, however, an inhomogeneous helical state has existed above that temperature due to the strong precursor phenomena[19,28]. The higher T_C determined here indicates the appearance of precursor phenomena which may be caused by the strong spin fluctuation[24]. Figure 1(b) shows the isothermal magnetization $M(H)$ at 4 K, which exhibits a typical magnetic ordering behavior. The inset of Fig. 1(b) plot the magnified $M(H)$ in lower field regime, which shows that the saturation field $H_S \approx 3000$ Oe. No magnetic hysteresis is found on the $M(H)$ curve, indicating no coercive force for FeGe.

Usually, the critical exponents can be determined by the Arrott plot. For the Landau mean-field model with $\beta = 0.5$ and $\gamma = 1.0$[29], the Arrott-Noakes equation of state evolves into $H/M = A + BM^2$, the so called Arrott equation. In order to construct an Arrot plot, the isothermal magnetization curves $M(H)$ around T_C are measured as shown in Fig. 2(a). The Arrott plot of M^2 vs H/M for FeGe is depicted in Fig. 2(b). According to the Banerjee's criterion, the slope of line in the Arrott plot indicates the order of the phase transition: negative slope corresponds to first-order transition while positive to second-order one[30]. Therefore, the Arrott plot of FeGe implies a second-order phase transition, in agreement with the specific heat measurement[28]. According to the Arrott plot, the M^2 vs H/M generally present a series of parallel straight lines around T_C, where H/M vs. M^2 at T_C just pass through the origin[31]. One can see that all M^2 vs H/M curves show quasi-straight lines with positive slopes in high field range. However, all lines show an upward curvature and are not parallel to each other, indicating that the $\beta = 0.5$ and $\gamma = 1.0$ within the framework of Landau mean-field model is unsatisfied. Therefore, a modified Arrott plot should be employed.

Four kinds of possible exponents belonging to the 3D-Heisenberg model ($\beta = 0.365$, $\gamma = 1.336$), 3D-Ising model ($\beta = 0.325$, $\gamma = 1.24$), 3D-XY model ($\beta = 0.345$, $\gamma = 1.316$), and tricritical mean-field model ($\beta = 0.25$, $\gamma = 1.0$)[29,32] are used to construct the modified Arrott plots, as shown in Fig. 3 (a–d). All these four constructions exhibit quasi-straight lines in the high field region[33–35]. Apparently, the lines in Fig. 3(d) are not parallel to each other, indicating that the tricritical mean-field model is not satisfied. However, all lines in Fig. 3(a–c) are almost parallel to each other. To determine an appropriate model, the modified Arrott plots should be a series of parallel lines in the high field region with the same slope, where the slope is defined as $S(T) = dM^{1/\beta}/d(H/M)^{1/\gamma}$. The normalized slope (*NS*) is defined as $NS = S(T)/S(T_C)$, which enables us to identify the most suitable model by comparing the *NS* with the ideal value of '1'[33]. Plots of *NS* vs *T* for the four different models are shown in Fig. 4. One can see that the *NS* of 3D-Heisenberg model is close to '1' mostly above T_C, while that of 3D-Ising model is the best below T_C. This result indicates that the critical behavior of FeGe may not belong to a single universality class.

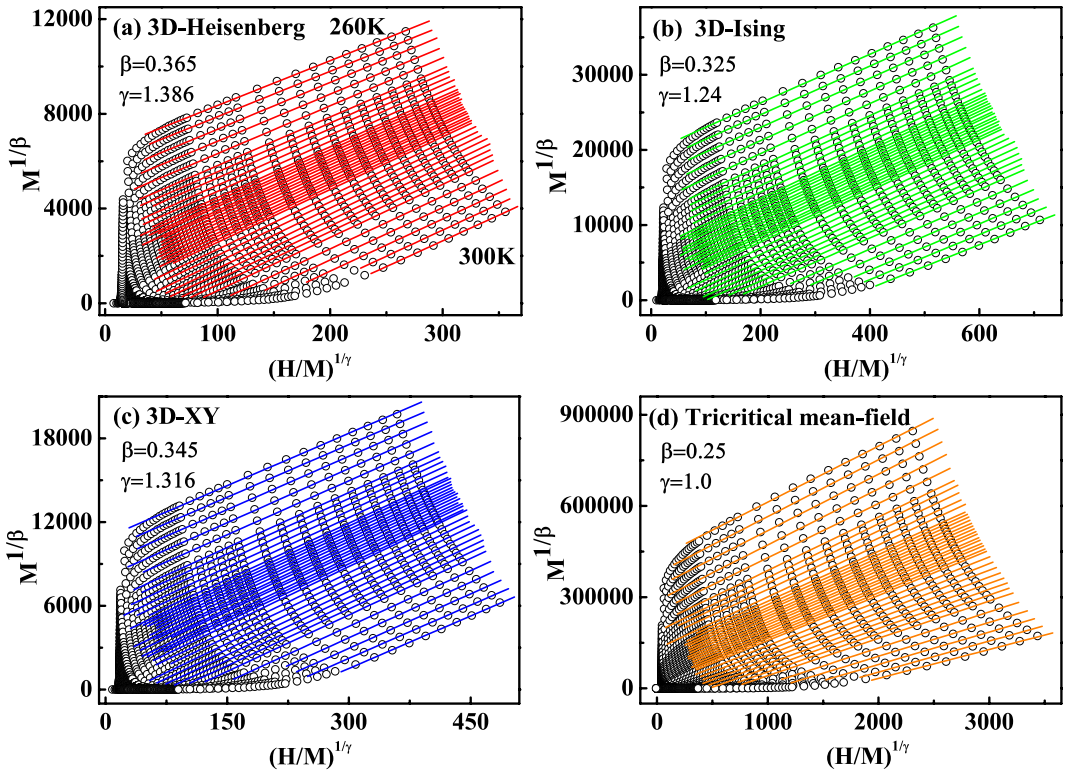

Figure 3. The isotherms of $M^{1/\beta}$ vs $(H/M)^{1/\gamma}$ with (**a**) 3D-Heisenberg model; (**b**) 3D-Ising model; (**c**) 3D-XY model; and (**d**) tricritical mean-field model.

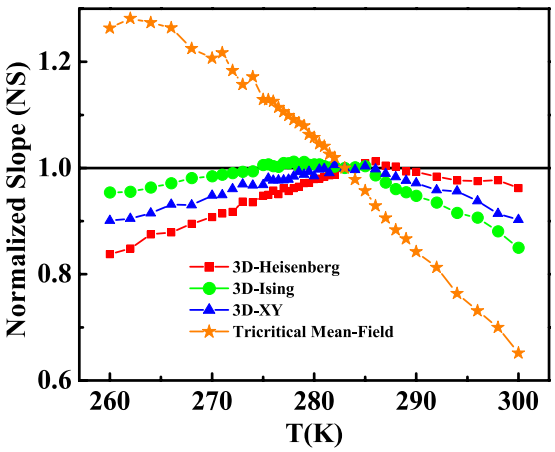

Figure 4. The normalized slopes [$NS = S(T)/S(T_C)$] as a function of temperature.

The precise critical exponents β and γ should be achieved by the iteration method[36]. The linear extrapolation from the high field region to the intercepts with the axes $M^{1/\beta}$ and $(H/M)^{1/\gamma}$ yields reliable values of $M_S(T,\ 0)$ and $\chi_0^{-1}(T,\ 0)$, which are plotted as a function of temperature in Fig. 5(a). By fitting to Eqs. (1) and (2), one obtains a set of β and γ. The obtained β and γ are used to reconstruct a new modified Arrott plot. Consequently, new $M_S(T,\ 0)$ and $\chi_0^{-1}(T,\ 0)$ are generated from the linear extrapolation from the high field region. Therefore, another set of β and γ can be yielded. This procedure is repeated until β and γ do not change. As one can see, the obtained critical exponents by this method are independent on the initial parameters, which confirms these critical exponents are reliable and intrinsic. In this way, it is obtained that $\beta = 0.336 \pm 0.004$ with $T_C = 283.18 \pm 0.05$ and $\gamma = 1.352 \pm 0.003$ with $T_C = 282.87 \pm 0.08$ for FeGe. The critical temperature T_C from the modified Arrott plot is in agreement with that obtained from the derivative $M(T)$ curve, indicating strong critical fluctuation before the formation of the long-range ordering in FeGe[24]. This critical fluctuation is in agreement with the precursor phenomenon reported by Wilhelm *et al.*[28]. The modulated precursor states and

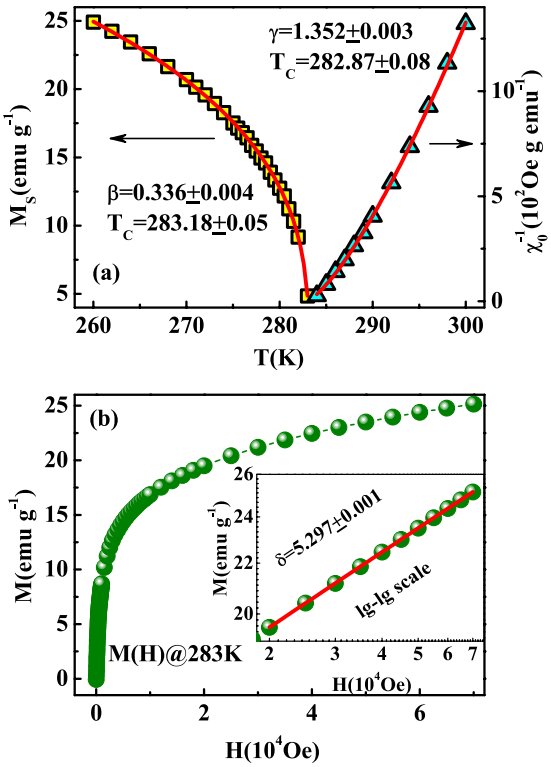

Figure 5. (**a**) The temperature dependence of M_S and χ_0^{-1} for FeGe with the fitting solid curves; (**b**) the isothermal $M(H)$ at T_C with the inset plane on lg − lg scale (the solid line is fitted).

complexity of the magnetic phase diagram near the magnetic ordering are explained by the change of the character of solitonic inter-core interactions and the onset of specific confined chiral modulations[19,28].

Figure 5(b) shows the isothermal magnetization $M(H)$ at the critical temperature $T_C = 283$ K, with the inset plotted on a lg − lg scale. One can see that the $M(H)$ at T_C exhibits a straight line on a lg − lg scale for $H > H_S$. We determine that $\delta = 5.297 \pm 0.001$ in the high field region ($H > H_S$). According to the statistical theory, these critical exponents should fulfill the Widom scaling law[37]:

$$\delta = 1 + \frac{\gamma}{\beta} \tag{5}$$

As a result, $\delta = 5.024 \pm 0.005$ is calculated according to the Widom scaling law, in agreement with the results from the experimental critical isothermal analysis. The self-consistency of the critical exponents demonstrates that they are reliable and unambiguous.

Finally, these critical exponents should obey the scaling equations. Two different constructions have been used in this work, both of which are based on the scaling equations of state. According to the scaling equations, in the asymptotic critical region, the magnetic equation is written as[25]:

$$M(H, \varepsilon) = \varepsilon^{\beta} f_{\pm}(H/\varepsilon^{\beta+\gamma}) \tag{6}$$

where $f_{\pm}$ are regular functions denoted as f_+ for $T > T_C$ and f_- for $T < T_C$. Defining the renormalized magnetization as $m \equiv \varepsilon^{-\beta} M(H, \varepsilon)$, and the renormalized field as $h \equiv H\varepsilon^{-(\beta+\gamma)}$, the scaling equation indicates that m vs h forms two universal curves for $T > T_C$ and $T < T_C$ respectively[38,39]. Based on the scaling equation [$m = f_{\pm}(h)$], the isothermal magnetization around T_C for FeGe is replotted in Fig. 6(a), where all experimental data collapse onto two universal branches. The inset of Fig. 6(a) shows he m^2 vs h/m, where all $M - T - H$ curves should collapse onto two independent universal curves. In addition, the scaling equation of state takes another form[25,38]:

$$\frac{H}{M^{\delta}} = k\left(\frac{\varepsilon}{H^{1/\beta}}\right) \tag{7}$$

where $k(x)$ is the scaling function. Based on Eq. (7), all experimental curves will collapse onto a single curve. Figure 6(b) shows the $MH^{-1/\delta}$ vs $\varepsilon H^{-1/(\beta+\gamma)}$ for FeGe, where the experimental data collapse onto a single curve, and T_C locates at the zero point of the horizontal axis. The well-rescaled curves further confirm the reliability of the obtained critical exponents.

The obtained critical exponents of FeGe and other related materials, as well as those from different theoretical models are summarized in Table 1 for comparison. One can see that the critical exponent γ of FeGe is close to that

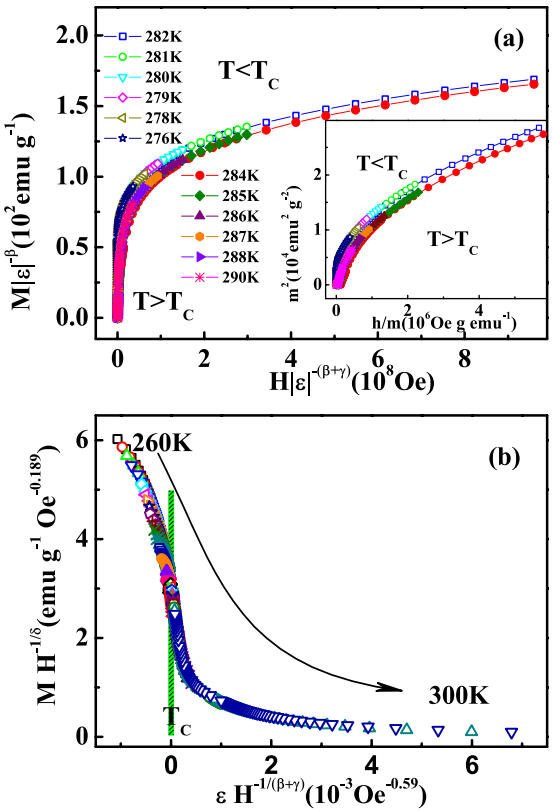

Figure 6. (**a**) Scaling plots of renormalized magnetization m vs renormalized field h around the critical temperatures for FeGe (the inset shows the m^2 vs h/m); (**b**) the rescaling of the the $M(H)$ curves by $MH^{-1/\delta}$ vs $\varepsilon H^{-1/(\beta+\gamma)}$.

Composition	technique	Ref.	T_C(K)	β	γ	δ
$FeGe^{PC}$	MAP	This work	283	0.336 ± 0.004	1.352 ± 0.003	5.267 ± 0.001
3D-Heisenberg	theory	29	–	0.365	1.386	4.8
3D-XY	theory	29	–	0.346	1.316	4.81
3D-Ising	theory	29	–	0.325	1.24	4.82
Tricritical mean-field	theory	32	–	0.25	1.0	5.0
Mean-field	theory	29	–	0.5	1.0	3.0
$MnSi^{SC}$	MAP	48	30.5	0.242 ± 0.006	0.915 ± 0.003	4.734 ± 0.006
$Fe_{0.8}Co_{0.2}Si^{PC}$	Hall	45	36.0	0.371 ± 0.001	1.38 ± 0.002	4.78 ± 0.01
$Cu_2OSeO_3^{SC}$	AC	46	58.3	0.37(1)	1.44(4)	4.9(1)

Table 1. Comparison of critical exponents of FeGe with different theoretical models and related materials (MAP = modified Arrott plot; Hall = Hall effect; AC = ac susceptibility; SC = single crystal; PC = polycrystal).

of 3D-Heisenberg model, while β approaches to that of 3D-Ising or 3D-XY mode, indicating that the critical behavior of FeGe do not belong to a single universality class. Anyhow, all these three models indicate a short-range magnetic coupling, implying the existence of short-range magnetic interaction in FeGe. As we know, for a homogeneous magnet, the universality class of the magnetic phase transition depends on the exchange distance $J(r)$. M. E. Fisher *et al.* have treated this kind of magnetic ordering as an attractive interaction of spins, where a renormalization group theory analysis suggests $J(r)$ decays with distance r as[40,41]:

$$J(r) \approx r^{-(d+\sigma)} \tag{8}$$

where d is the spatial dimensionality and σ is a positive constant. Moreover, there is[41,42]:

$$\gamma \approx 1 + \frac{4}{d}\frac{n+2}{n+8}\Delta\sigma + \frac{8(n+2)(n-4)}{d^2(n+8)^2}\left[1 + \frac{2G\left(\frac{d}{2}\right)(7n+20)}{(n-4)(n+8)}\right]\Delta\sigma^2 \quad (9)$$

where $\Delta\sigma = \left(\sigma - \frac{d}{2}\right)$ and $G\left(\frac{d}{2}\right) = 3 - \frac{1}{4}\left(\frac{d}{2}\right)^2$, n is the spin dimensionality. For a three dimensional material ($d = 3$), we have $J(r) \approx r^{-(3+\sigma)}$. When $\sigma \geq 2$, the Heisenberg model ($\beta = 0.365, \gamma = 1.386$ and $\delta = 4.8$) is valid for the three dimensional isotropic magnet, where $J(r)$ decreases faster than r^{-5}. When $\sigma \leq 3/2$, the mean-field model ($\beta = 0.5, \gamma = 1.0$ and $\delta = 3.0$) is satisfied, expecting that $J(r)$ decreases slower than $r^{-4.5}$. From Eq. (9) $\sigma = 1.908 \pm 0.007$ is generated for FeGe, thus close to the short-range magnetic coupling of $\sigma \sim 2$. Subsequently, it is found that the magnetic exchange distance decays as $J(r) \approx r^{-4.9}$, which indicates that the magnetic coupling in FeGe is close to a short-range interaction. Moreover, we get the correlation length critical exponent $\nu = 0.709 \pm 0.008$ (where $\nu = \gamma/\sigma$, $\xi = \xi_0|(T - T_C)/T_C|^{-\nu}$), and $\alpha = (2 - \nu d) = -1.127 \pm 0.008$. Theory gives that $\alpha = -0.115(9)$ for 3D-Heisenberg model and $\alpha = 0.110(5)$ for 3D-Ising model[43,44]. Therefore, these critical exponents indicates that the critical behavior in FeGe is close to the 3D-Heisenberg model with short-range magnetic coupling. However, the discrepancy of the critical exponents to 3D-Ising or 3D-XY models indicates an anisotropic magnetic exchange interaction.

As can be seen from Table 1, the critical exponents of $Fe_{0.8}Co_{0.2}Si$ and Cu_2OSeO_3, which also exhibit a helimagnetic and skyrmion phase transition with similar crystal symmetry, are close to the universality class of the 3D-Heisenberg model[45,46], indicating a isotropic short-range magnetic coupling. However, the critical behavior of MnSi belongs to the tricritical mean field model[47,48]. In macroscopic view, the magnetic ordering in cubic FeGe is a DM spiral similar to the structure observed in the isostructural compound MnSi[49]. However, in microscopic view, the magnetic coupling types in these two helimagnets are different. The critical behavior of FeGe is roughly similar to those of $Fe_{0.8}Co_{0.2}Si$ or Cu_2OSeO_3, except a magnetic exchange anisotropy. In MnSi the spiral propagates are along equivalent <111> directions at all temperatures below $T_C = 29.5$ K. However, it has been revealed that the helical axis ($q-$vector direction) in FeGe depends on temperature. It is along the <001> direction below 280 K, and changes to the <111> direction in a lower temperature range at 211 K with the decrease of temperature at zero magnetic field[20]. This unique change of helical axis in FeGe may be correlated with the anisotropy of magnetic exchange in this system, since the magnetic exchange anisotropy also plays an important role in determination of the spin ordering direction. In addition, it should be expounded that the magnetic exchange anisotropy is essentially different from the magnetocrystalline anisotropy. The magnetocrystalline anisotropy is correlated to the crystal structure, while magnetic exchange anisotropy originates from the anisotropic magnetic exchange coupling J.

Conclusion

In summary, the critical behavior of the near room temperature skyrmion material FeGe has been investigated around T_C. The reliable critical exponents ($\beta = 0.336 \pm 0.004, \gamma = 1.352 \pm 0.003$, and $\delta = 5.267 \pm 0.001$) are obtained, which are verified by the Widom scaling law and scaling equations. The magnetic exchange distance is found to decay as $J(r) \approx r^{-4.9}$, which is close to that of 3D-Heisenberg model (r^{-5}). The critical behavior indicate that the magnetic interaction in FeGe is of short-range type with an anisotropic magnetic exchange coupling.

Methods

A polycrystalline B20-type FeGe sample was synthesized with a cubic anvil-type high-pressure apparatus. The detailed preparing method was described elsewhere, and the physical properties were carefully checked [H. Du. *et al.*, Nat. Commun. **6**, 8504 (2015)]. The chemical compositions were determined by the Energy Dispersive X-ray (EDX) Spectrometry as shown in Fig. S1 and Table S I, which shows the atomic ratio of Fe : Ge ≈ 50.52: 49.48. The magnetization was measured using a Quantum Design Vibrating Sample Magnetometer (SQUID-VSM). The no-overshoot mode was applied to ensure a precise magnetic field. To minimize the demagnetizating field, the sample was processed into slender ellipsoid shape and the magnetic field was applied along the longest axis. In addition, the isothermal magnetization was performed after the sample was heated well above T_C for 10 minutes and then cooled under zero field to the target temperatures to make sure curves were initially magnetized. The magnetic background was carefully subtracted. The applied magnetic field H_a has been corrected into the internal field as $H = H_a - NM$ (where M is the measured magnetization and N is the demagnetization factor) [A. K. Pramanik *et al.*, Phys. Rev. B **79**, 214426 (2009)]. The corrected H was used for the analysis of critical behavior.

References

1. Roβler, U. K., Bogdanov, A. N. & Pfleiderer, C. Spontaneous skyrmion ground states in magnetic metals. *Nature (London)* **442,** 797–801 (2006).
2. Muuhlbauer, S. *et al.* Skyrmion lattice in a chiral magnet. *Science* **323,** 915–919 (2009).
3. Munzer, W. *et al.* Skyrmion lattice in the doped semiconductor $Fe_{1-x}Co_xSi$. *Phys. Rev. B* **81,** 041203 (2010).
4. Yu, X. Z. *et al.* Real-space observation of a two-dimensional skyrmion crystal. *Nature (London)* **465,** 901–904 (2010).
5. Seki, S., Yu, X. Z., Ishiwata, S. & Tokura, Y. Observation of skyrmions in a multiferroic material. *Science* **336,** 198–201 (2012).
6. Du, H. F., Ning, W., Tian, M. L. & Zhang, Y. H. Field-driven evolution of chiral spin textures in a thin helimagnet nanodisk. *Phys. Rev. B* **87,** 014401 (2013).
7. Neubauer, A. *et al.* Topological Hall effect in the A phase of MnSi. *Phys. Rev. Lett.* **102,** 186602 (2009).
8. Du, H. F. *et al.* Highly stable skyrmion state in helimagnetic MnSi nanowires. *Nano Lett.* **14,** 2026–2032 (2014).
9. Nagaosa N. & Tokura, Y. Topological properties and dynamics of magnetic skyrmions. *Nat. Nanotechnol.* **8,** 899–911 (2013).
10. Jonietz, F. *et al.* Spin transfer torques in MnSi at ultralow current densities. *Science* **330,** 1648–1651 (2010).
11. Fert, A., Cros, V. & Sampaio, J. Skyrmions on the track. *Nat. Nanotechnol.* **8,** 152–156 (2013).

12. White, J. S. *et al.* Electric-field-induced skyrmion distortion and giant lattice rotation in the magnetoelectric insulator Cu_2OseO_3. *Phys. Rev. Lett.* **113,** 107203 (2014).
13. Bogdanov, A. & Yablonsky, D. Thermodynamically stable vortexes in magnetically ordered crystals-mixed state of magnetics. *Sov. Phys. JETP* **96,** 253 (1989).
14. Bogdanov, A. & Hubert, A. Thermodynamically stable magnetic vortex states in magnetic crystals. *J. Magn. Magn. Mater.* **138,** 255–269 (1994).
15. Romming, N. *et al.* Writing and deleting single magnetic skyrmions. *Science* **341,** 636–639 (2013).
16. Romming, N., Kubetzka, A., Hanneken, C., von Bergmann, K. & Wiesendanger, R. Field-dependent size and shape of single magnetic skyrmions. *Phy. Rev. Lett*. **114,** 177203 (2015).
17. Yu, X. Z. *et al.* Skyrmion flow near room temperature in an ultralow current density. *Nat. Commun.* **3,** 988 (2012).
18. Bak, P. & Jensen, M. H. Theory of helical magnetic structures and phase transitions in MnSi and FeGe. *J. Phys. C: Solid St. Phys*. **13,** L881 (1980).
19. Wilhelm, H. *et al.* Precursor phenomena at the magnetic ordering of the cubic helimagnet FeGe. *Phys. Rev. Lett.* **107,** 127203 (2011).
20. Lebech, B., Bernhard, J. & Freltoft, T. Magnetic structures of cubic FeGe studied by small-angle neutron scattering. *J. Phys. Condens. Matter* **1,** 6105–6122 (1989).
21. Yu, X. Z. *et al.* Near room-temperature formation of a skyrmion crystal in thin-films of the helimagnet FeGe. *Nat. Mater.* **10,** 106–109 (2011).
22. Shibata, K. *et al.* Large anisotropic deformation of skyrmions in strained crystal. *Nat. Naonotechol.* **10,** 589–592 (2015).
23. Koretsune, T., Nagaosa, N. & Arita, R. Control of Dzyaloshinskii-Moriya interaction in $Mn_{1-x}Fe_xGe$: a first-principles study. *Sci. Rep*. **5,** 13302 (2015).
24. Barla, A. *et al.* Pressure-induced inhomogeneous chiral-spin ground state in FeGe. *Phys. Rev. Lett.* **114,** 016803 (2015).
25. Stanley, H. E. *Introduction to Phase Transitions and Critical Phenomena* (Oxford University Press, London, 1971).
26. Fisher, M. E. The theory of equilibrium critical phenomena. *Rep. Prog. Phys.* **30,** 615–730 (1967).
27. Arrott, A. & Noakes, J. Approximate equation of state for Nickel near its critical temperature. *Phys. Rev. Lett.* **19,** 786 (1967).
28. Wilhelm, H. *et al.* Confinement of chiral magnetic modulations in the precursor region of FeGe. *J. Phys. Condens. Matter* **24,** 294204 (2012).
29. Kaul, S. N. Static critical phenomena in ferromagnets with quenched disorder. *J. Magn. Magn. Mater.* **53,** 5–53 (1985).
30. Banerjee, S. K. On a generalised approach to first and second order magnetic transitions. *Phys. Lett.* **12,** 16–17 (1964).
31. Arrott, A. Criterion for ferromagnetism from observations of magnetic isotherms. *Phys. Rev.* **108,** 1394–1396 (1957).
32. Huang, K. *Statistical Mechanics* 2nd ed. (Wiley, New York, 1987).
33. Fan, J. Y. *et al.* Critical properties of the perovskite manganite $La_{0.1}Nd_{0.6}Sr_{0.3}MnO_3$. *Phys. Rev. B* **81,** 144426 (2010).
34. Zhang, L. *et al.* Critical behavior in the antiperovskite ferromagnet $AlCMn_3$. *Phys. Rev. B* **85,** 104419 (2012).
35. Zhang, L. *et al.* Critical properties of the 3D-Heisenberg ferromagnet $CdCr_2Se_4$. *Europhys. Lett.* **91,** 57001 (2010).
36. Zhang, L. *et al.* Critical behavior of single crystal $CuCr_2Se_{4-x}Br_x$ ($x = 0.25$). *Appl. Phys. A* **113,** 201–206 (2013).
37. Kadanoff, L. P. Scaling laws for Ising models near T_C. *Physics* **2,** 263–272 (1966).
38. Phan, M. H. *et al.* Tricritical point and critical exponents of $La_{0.7}Ca_{0.3-x}Sr_xMnO_3$ ($x = 0$, 0.05, 0.1, 0.2, 0.25) single crystals. *J. Alloys Compd.* **508,** 238–244 (2010).
39. Khan, N. *et al.* Critical behavior in single-crystalline $La_{0.67}Sr_{0.33}CoO_3$. *Phys. Rev. B* **82,** 064422 (2010).
40. Ghosh, K. *et al.* Critical phenomena in the double-exchange ferromagnet $La_{0.7}Sr_{0.3}MnO_3$. *Phys. Rev. Lett.* **81,** 4740 (1998).
41. Fisher, M. E., Ma, S. K. & Nickel, B. G. Critical exponents for long-range interactions. *Phys. Rev. Lett.* **29,** 917–920 (1972).
42. Fischer, S. F., Kaul, S. N. & Kronmuller, H. Critical magnetic properties of disordered polycrystalline $Cr_{75}Fe_{25}$ and $Cr_{70}Fe_{30}$ alloys. *Phys. Rev. B* **65,** 064443 (2002).
43. Fisher, M. E. The renormalization group in the theory of critical behavior. *Rev. Mod. Phys.* **46,** 597–616 (1974).
44. LeGuillou J. C. & Zinn-Justin, J. Critical exponents from eld theory. *Phys. Rev. B* **21,** 3976–3998 (1980).
45. Jiang, W. J., Zhou, X. Z. & Williams, G. Scaling the anomalous Hall effect: A connection between transport and magnetism. *Phys. Rev. B* **82,** 144424 (2010).
46. Zivkovic, I., White, J. S., Ronnow, H. M., Prsa, K. & Berger, H. Critical scaling in the cubic helimagnet Cu_2OseO_3. *Phys. Rev. B* **89,** 060401(R) (2014).
47. Bauer, A., Garst, M. & Pfleiderer, C. Specific heat of the skyrmion lattice phase and field-induced tricritical point in MnSi. *Phys. Rev. Lett.* **110,** 177207 (2013).
48. Zhang, L. *et al.* Critical behavior of the single-crystal helimagnet MnSi. *Phys. Rev. B* **91,** 024403 (2015).
49. Bauer, A. & Pfleiderer, C. Magnetic phase diagram of MnSi inferred from magnetization and ac susceptibility. *Phys. Rev. B* **85,** 214418 (2012).

Acknowledgements

This work was supported by the State Key Project of Fundamental Research of China through Grant No. 2011CBA00111, the National Natural Science Foundation of China (Grant Nos 11574322, U1332140, 11004196, U1232142, 11474290, 11104281, and 11204288), the Foundation for Users with Potential of Hefei Science Center (CAS) through Grant No. 2015HSC-UP001 the Youth Innovation Promotion Association CAS No.2015267.

Author Contributions

Y.H.Z. conducted the analyses. L.Z. conducted all of the experiments and wrote the paper. H.F.D., C.M.J. and W.S.W. synthesized the sample. H.H. collected the EDX spectrum. M.G. performed the magnetic measurements. J.Y.F., C.J.Z. and L.P. analyzed the experimental results.

Additional Information

Supplementary information accompanies this paper at http://www.nature.com/srep

Competing financial interests: The authors declare no competing financial interests.

How to cite this article: Zhang, L. *et al.* Critical phenomenon of the near room temperature skyrmion material FeGe. *Sci. Rep.* **6**, 22397; doi: 10.1038/srep22397 (2016).